Surfactant effect and dissolution of ultrathin Fe films on Ag(001)

S. Terreni,[1] A. Cossaro,[2] G. Gonella,[1] L. Mattera,[1] L. Duò,[3] F. Ciccacci,[3] D. Cvetko,[2,*] L. Floreano,[2] A. Morgante,[2,†] A. Verdini,[2] and M. Canepa[1,‡]

[1]*Unità INFM and CNR-IMEM, Dipartimento di Fisica, Università di Genova, via Dodecaneso 33, I-16146 Genova, Italy*

[2]*Laboratorio TASC-INFM, Trieste, Italy*

[3]*INFM and Dipartimento di Fisica, Politecnico di Milano, Italy*

(Received 31 December 2003; revised manuscript received 25 May 2004; published 29 September 2004)

The effects of annealing on the structure of ultra thin Fe films (4–10 ML) deposited at 150 K on Ag(001) were studied by synchrotron radiation photoelectron diffraction (PED) and x-ray diffraction (XRD). The occurrence of a surfactant-like stage, in which a single layer of Ag covers the Fe film is demonstrated for films of 4–6 ML heated at 500–550 K. Evidence of a stage characterized by the formation of two Ag capping layers is also reported. As the annealing temperature was increased beyond 700 K the surface layers closely resembled the structure of bare Ag(001) with the residual presence of subsurface Fe aggregates. The data illustrate a film dissolution path which is in agreement with recent theoretical models [J. Roussel *et al.* Phys. Rev. B **60**, 13890 (1999)].

DOI: 10.1103/PhysRevB.70.115420 PACS number(s): 68.35.−p, 68.55.−a

The phase immiscibility and the excellent matching between Ag(001) and Fe(001) unit cells (mismatch 0.8%) make Fe/Ag growth attractive in the field of low dimensionality magnetic systems, such as ultrathin films,[1] multilayers,[2] and small aggregates.[3] At the nanometric scale, atomic exchange processes were found to affect the chemical sharpness of interfaces in films and multilayers.[4] Intermixing could be drastically limited at deposition temperatures as low as 140–150 K[4–6] at the expense of a poor morphological quality of the film.[7,8] The film structural evolution induced by post-growth annealing presents many interesting aspects involving activated atomic exchange processes and affecting magnetic properties.[9] Previous experiments, of He and low energy ion scattering on films deposited at 150 K, indicated the formation of a segregated Ag layer upon moderate annealing (550 K). Higher temperatures led to the embedding of Fe into the Ag matrix.[10] These processes resemble the encapsulation of Rh, Pt and Pd clusters into Cu and Ag surfaces reported by Thiel and coworkers.[11] The formation of pin-holes extending down to the substrate has been suggested as a precursor stage of the encapsulation process,[12,13] enabling upward exchange diffusion of substrate atoms to the film surface.[14] Regarding the Fe/Ag system, we obtained information on the subsurface layers composition by ion erosion depth profiling, a destructive technique.[10] Due to the limited probing depth of previous investigations, many questions remained open about the structure of the buried film and its morphology evolution during dissolution. Here we address this issue by presenting photoelectron and x-ray diffraction experiments (PED and XRD, respectively), performed at the ALOISA beam line (ELETTRA, Trieste). PED provides chemical state specific data on film structure with an information depth of several layers. It allows us to characterize local order in films which are disordered on a long range scale and possesses specific sensitivity to segregation processes.[15] Systematic PED measurements have been accompanied with a few XRD rod scans yielding a better sensitivity to the buried interface and the film long range order.

The results of this paper allow a comparison with recent models enlightening the temperature-induced surfactant-like effect and the dissolution paths of an ultra thin metal film into a different metal, when both subsurface migration of the deposit and phase separation between substrate and deposit are favored.[22,23]

Details on the ALOISA system can be found elsewhere.[16] The Ag substrate was prepared according to well established procedures.[7] Reflection High Energy Electron Diffraction was used to monitor the surface order. XPS surveys were employed to check the chemical composition of the surface. Grazing incidence XPS was also used to monitor in real time Fe $2p$ and Ag $3p$ signals during annealing ramps. The sample temperature was controlled by thermocouples and by an optical pyrometer. Iron was evaporated by electron bombardment, controlling the deposition flux ($\sim$1.5 Å/min) by a quartz microbalance. Attention was focused on films in the 4–10 ML thickness range deposited at 150 K. After deposition the films were annealed up to the desired temperature, then immediately cooling the system for the measurements. We address the reader to Ref. 10 for a detailed discussion of the annealing protocol adopted. Grazing incidence XRD has been taken on a few films by measuring radial scans across the $(\bar{2}00)$ and $(2\bar{2}0)$ peaks in the in–plane Ag(001) reciprocal lattice. These measurements yielded the lateral lattice spacing with a precision of better than 0.01 Å. The vertical structure of the pseudomorphic Fe film has been also probed by out-of-plane XRD (rod scan). The $(\bar{2}0L)$ rods of the Ag(001) substrate were taken at grazing angle with a photon energy of 6000 eV. For each L value, an azimuthal scan of the sample was performed in order to collect the whole diffracted intensity. The simulations of the rod scans were performed by the Vlieg's program ROD.[17] PED polar scans were measured at grazing incidence ($h\nu$=900–1300 eV, p polarization) by rotating an electron energy analyzer in the scattering plane. The notation Ag (Fe) $nl(\theta)$, will indicate PED scans as a function of the polar angle θ from the surface normal, obtained by photoemission from nl states of Ag (Fe). The pho-

toemission intensity was collected at the peak energy and at suitably chosen energies along the peak tails in order to allow for a subtraction of the background due to secondary electrons. FF will denote forward focusing peaks along off normal nearest neighbor atomic chains. For the sake of synthesis we will only show data taken with the ⟨001⟩ Ag surface direction in the scattering plane.

The computational approach to PED has been thoroughly described elsewhere.[18] In brief, the polar scans $I_{exp}(\theta)$ have been compared with calculated $I_{calc}(\theta) = ISO_{calc}(\theta)(1+\chi_{calc}(\theta))$. The anisotropy term $\chi_{calc}(\theta)$, carrying information on the arrangement of atoms around the photo-emitter, was taken proportional to the output generated by the Multiple Scattering Calculation of Diffraction (MSCD) package.[19] Several structural models have been considered both for the as-deposited and the annealed films. We varied the number of Fe planes and considered the presence of one or more Ag layers over the Fe film; intermixed interfaces were also examined. In all calculations, the in-plane lattice constants of the film a_{Fe} was set to the substrate value $a_{Ag}=2.88$ Å, inferred from in-plane grazing incidence XRD, which indicated a pseudomorphic in-plane structure, independently on the investigated thickness and annealing temperature. In fact, the formation of a nonpseudomorphic Fe film would have yielded side-peaks or shoulders close to the substrate in-plane XRD peaks,[20] which were never observed. The isotropic term $ISO_{calc}(\theta)$ has been calculated, taking into account emission matrix elements, electron escape path, surface roughness and instrumental factors.[18] Regarding as-deposited films, systematic PED (and Auger electron diffraction) measurements, taken along several azimuthal orientations, indicated the growth of Fe films with a body centered cubic structure and unit cell rotated by 45° with respect to the substrate cell (in brief ^{R45}bcc structure). The body of data resulted in close agreement with literature.[4,21] For films thicker than 5 ML the ratio between the vertical and in-plane lattice constants c_{Fe}/a_{Fe} matched unity, as expected for an ideal bcc structure. On the thinnest films the FF peak was slightly shifted from the bcc position, giving a value $c_{Fe}/a_{Fe}=1.06\pm0.01$ for a 4 ML film. This expansion of c_{Fe} was early attributed to the influence of intermixing at the interface.[4,7] Representative measurements on a 6 ML film are reported in the upper panel of Fig. 1.

In the figure, the simulations were generated employing a model with 6 layers of Fe (^{R45}bcc structure) laying on the substrate mimicked by 3 layers of Ag (in brief 6Fe/Sub). Concerning the Fe pattern, the simulation was insensitive to the value of the interlayer distance at the interface (d_{Ag}^{Fe}). The best simulation of the Ag $3p$ (θ) pattern, showing a strong attenuation of intensity and significant shape variations with respect to the bare Ag(001), was obtained with $d_{Ag}^{Fe}=1.70\pm0.03$ Å. This value, in between Ag ($d_{Ag}\sim2.04$ Å) and Fe ($d_{Fe}\sim1.43$ Å) bulk interlayer spacings, enabled the reproduction of the main features of the pattern, including the suppression of the FF peak typical of the fcc structure, at 45°.

Fe $2p$ (θ) and Ag $3p$ (θ) patterns obtained on the same 6 ± 0.5 ML Fe film after annealing at 550 K are shown in the lower panel of Fig. 1. The shape of the Fe PED pattern

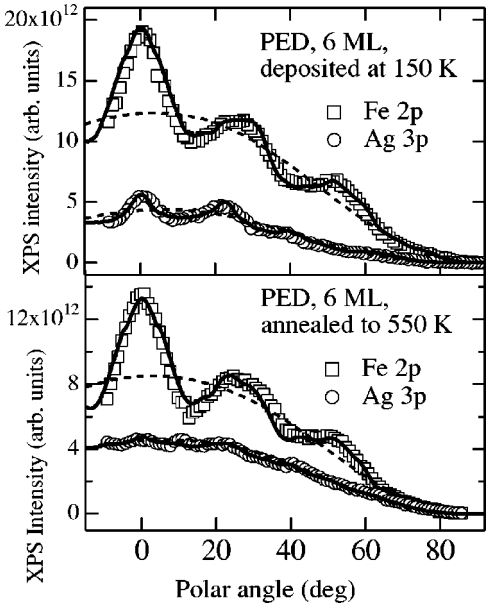

FIG. 1. Fe $2p$ (θ) and Ag $3p$ (θ) PED patterns obtained on a 6 ± 0.5 ML Fe film (upper panel) deposited at 150 K and (lower panel) after annealing at 550 K. Measurements were taken at 150 K along the ⟨100⟩ azimuth of the Ag substrate. In both panels continuous and dashed lines represent the calculated $I_{calc}(\theta)$ and ISO_{calc} patterns, respectively.

was similar to the as-deposited one. The Ag $3p$ (θ) data, showing a quasi isotropic behavior suggested the simple physical model of a Ag overlayer. Continuous lines in the figure were calculated according to a 1Ag/6Fe/Sub scheme. The structure of the Fe film was the same as used for the as-deposited film. The two Fe/Ag interfaces were assumed sharp. The Fe/Ag distance at the top layer resulted in $d_{Fe}^{Ag}=1.70\pm0.03$ Å.

The simulations reproduce rather accurately both Fe and Ag patterns supporting quantitatively the assumed structural model. A careful inspection of the data shows that the isotropic part of the Ag pattern did not change significantly with respect to the as-deposited film. Apart from experimental uncertainties, this finding can be rationalized in terms of interface roughness effects and possible incomplete Ag occupancy of the surface layer, as suggested by XRD measurements.

In this respect, the out-of-plane XRD scans along the $(\bar{2}0L)$ rod are shown in Fig. 2 for a 5 ± 0.5 ML Fe film, as taken for the just deposited (150 K) film and after annealing at 500 K and 750 K. The lack of interference modulations, related to the finite thickness of the as deposited film, is a fingerprint of a chemically smeared interface and surface roughness.[7] Well defined interference fringes appeared after annealing to 500 K witnessing the formation of a pseudomorphic film with smooth and sharp interfaces. It is therefore conceivable that in this case, the main contribution to the Ag PED signal comes from the surfactant layer and the contribution from substrate photoemitters is more efficiently attenuated.

Fitting to the rod scan of the annealed film yielded a model with 4.5 Fe layers covered by one Ag layer, thus act-

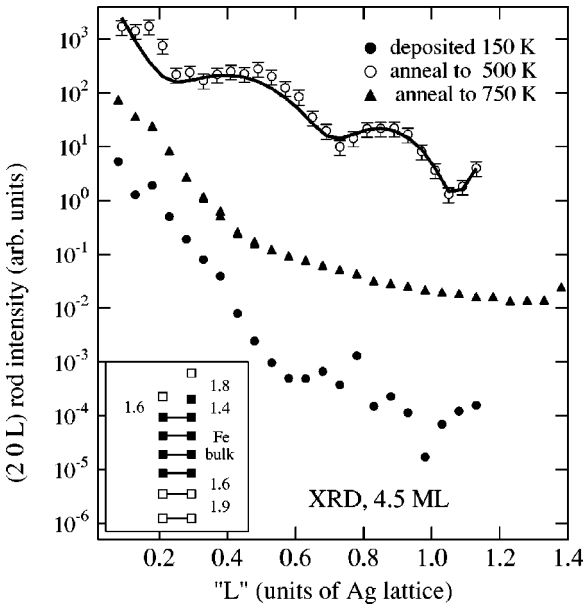

FIG. 2. XRD scan of the $(\bar{2}0L)$ rod of Ag for a 5 ± 0.5 ML Fe film. Measurements taken after the deposition and after annealing at different temperatures are shown. Modulations in the upper pattern arise from the formation of sharp interfaces at both top and bottom of the film. Fitting to the data (thick full line) yielded the structural model sketched in the inset, where filled and open squares represent the Fe and Ag layers, respectively. The topmost Ag layer is half filled, and the layer beneath is formed by 1/2 ML of Fe and 1/2 ML of Ag. Best fit layer spacings are also reported (in Å).

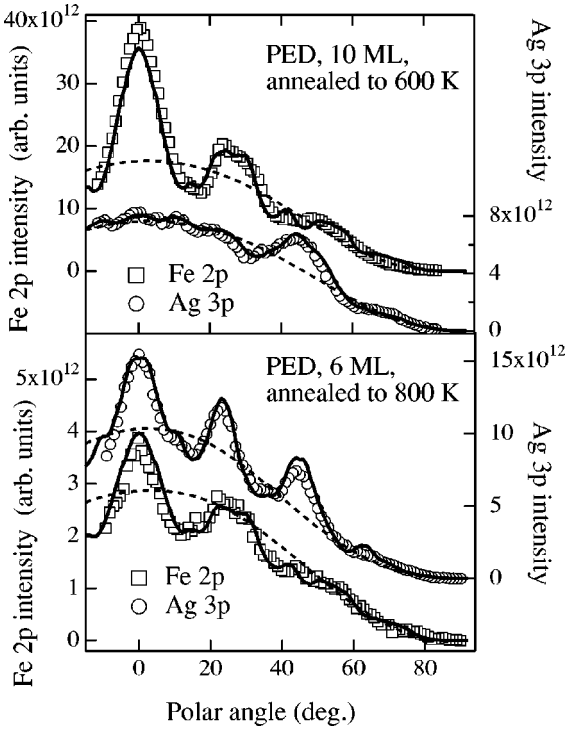

FIG. 3. Upper panel: Fe2$p(\theta)$ (squares) and Ag2$p(\theta)$ (circles) PED patterns on a 10 ± 0.5 ML Fe film deposited at 150 K and annealed to 600 K. Measurements were taken at 170 K along the $\langle 100\rangle$ azimuth of the Ag substrate. Fe and Ag intensity are reported in the left and right axis, respectively. Continuous and dashed lines represent the calculated $I_{calc}(\theta)$ and ISO_{calc} patterns, respectively, as described in the text. Lower panel: as in the upper panel, but for a 6 ± 0.5 ML Fe film after annealing at 800 K.

ing like an after-growth surfactant. Due to the limited region of reciprocal space explored, we considered a simple model with a few free parameters. In the model, the three spacings between the Fe layers from the 1st to the 4th one were fixed to the bulk spacing. We applied fitting optimization to the film interfaces which mostly affect the rod modulations. We found an height of 1.6 and 1.8 Å for the Ag surfactant layer above the 4th and 5th Fe layers, respectively. This discrepancy is simply due to the model simplification, where we have not allowed the relaxation of the 4th to 3rd Fe layer spacing (see the inset of Fig. 2). The width of the buried Fe-Ag interface was found to be 1.6 Å. The height of the first Ag layer below the Fe film was contracted to 1.9 Å. The same quality fits were obtained by admitting intermixing at the first Ag layer below the Fe film (10–15%). In this case the buried interface width was also slightly affected (uncertainty of 0.1 Å).

In the upper panel of Fig. 3, we show PED data obtained on a 10 ± 0.5 ML Fe film measured after annealing at 600 K. Fe $2p$ (θ) continued to show a bcc-like structure, but with an increased anisotropy along the normal direction. The Ag $3p$ (θ) data show faint features at 0°, ~10°, ~20° and a huge peak at 44°, indicating the formation of two Ag surfactant layers. The addition of a second Ag surface layer together with optimization of the d_{Fe}^{Ag} distance at the interface and of the d_{Ag}^{Ag} distance between the first and second Ag layer, yielded a satisfactory simulation of the Ag PED pattern. The I_{calc} curves, superimposed to the data of Fig. 3, were calculated considering a 2Ag/7Fe model with $d_{Fe}^{Ag}=1.73\pm0.03$ Å and $d_{Ag}^{Ag}=1.90\pm0.03$ Å. d_{Fe}^{Fe} was set at 1.43 Å. The simulation of the Fe $2p$ data was less satisfactory suggesting that the model oversimplifies the physical situation, where the second Ag layer could be only partially filled.

Upon further increasing the annealing temperature, the Ag $3p$ PED patterns gradually approached the one obtained on bare Ag(001). Representative data obtained on the 6 ± 0.5 ML film after annealing at 800 K are shown in the lower panel of Fig. 3. The Ag pattern was reproduced considering the same structural model used to fit the PED taken on the clean substrate (not shown), where at least five Ag layers are necessary to fit the pattern anisotropy. The overall intensity of the Fe $2p$ pattern presented an appreciable attenuation with respect to the as-deposited film, as well as to the film annealed at 600 K. However, significant anisotropy can still be detected. These findings suggested the presence of subsurface largely spaced Fe aggregates of small lateral size. Similar effects were also observed from XRD, where the rod scan taken after annealing to 750 K (filled triangles in Fig. 2) yielded a smooth decay due to the disruption of the subsurface Fe film. This rod scan is indicative of either Fe dissolution in the Ag matrix or fragmentation of the Fe film into small clusters of irregular size and spatial distribution. In order to get more information on such aggregates from PED data, we explored simple NAg/MFe structural models in which M layers of Fe (for simplicity with a

bcc structure) were buried below N layers of Ag (with interlayer distance d_{Ag}^{Ag}). A sharp Fe/Ag interface was considered with interface spacing d_{Fe}^{Ag}. In the case $M=6$, i.e., assuming for aggregates the same nominal thickness of the as-deposited film, a qualitative agreement (not shown) could be obtained with $N=1$ or 2. The agreement became definitely worse with larger values of N. Upon ~800 K annealing, the geometrical model describing the Ag PED pattern (five or more Ag layers on Fe) did not fit to the Fe PED pattern at all. The latter was fairly fitted by a 2Ag/8Fe model, $d_{Ag}^{Ag}=1.87\pm0.03$ Å, $d_{Fe}^{Ag}=1.67\pm0.03$ Å (full lines in Fig. 3). Thus, the analysis of a PED pattern confirms, on a quantitative ground, the residual presence of subsurface Fe clusters. While we have no indications about the cluster size, a Fe occupancy of ~0.1 can be estimated from the ratio of the Fe 2p intensities between the 800 and 600 K annealed films (in the latter case, the Fe film, covered by two Ag layers, seems not yet fragmented).

Our data can be rationalized in light of recent theories on the dissolution of ultra thin metal film into a metal substrate which enlightened different routes depending on the physical-chemical coupling of the deposit (A) and substrate (B).[22,23] When A and B present a tendency to bulk ordering, the dissolution can be blocked by the formation of AB surface alloys. In case of a tendency to A/B phase separation, dissolution paths will critically depend on the A and B surface energies. The case of interest here, in which B atoms show a stronger tendency to surface segregation than A atoms as for Fe/Ag or Ni/Ag systems,[24] was illustrated in Ref. 23 on the example of a 10 ML deposit (schematically indicated as A/A/$\cdots$/A/B). According to calculations, if the temperature is raised beyond a threshold T_C, dissolution proceeds through the so called surfactant-layer-by-layer (SLBLD) mode. In this regime, on a short range time scale, the system passes through a surfactant like stage, with the formation of successive B/A/A/$\cdots$/A/B, B/B/A/A/$\cdots$/A/B and B/B/B/A/A/$\cdots$/A/B profiles. The excellent agreement between the data of Figs. 1 and 2 with a 1 Ag/Fe/Fe/$\cdots$/Fe/Sub model nicely demonstrates the occurrence of the B/A/A/../A/B stage. Note that the MSCD simulations provide a reliable indication that the local structure of the Fe film remains substantially intact, in agreement with the model which predicts a negligible loss of deposit matter into the bulk at this stage.[23] In addition, XRD rod scans indicate that the formation of the first Ag surfactant layer does not involve a fragmentation of the Fe film. Rather the film is ordered to a uniform thickness in the early annealing stage and this order is preserved during the segregation of the first surfactant layer. Data of Fig. 3 (upper panel), representing a physical situation mimicking the B/B/A/$\cdots$/A/B stage, add further confidence about the agreement of our results with the model. The data of Fig. 3 (lower panel) illustrate a clear trend towards film dissolution, which appears in qualitative agreement with the final stage predicted by theory, i.e., the total disappearance of deposit species down to the tenth substrate layer, for $T>T_C$. Residual Fe clusters in the PED data for the highest annealing temperature is the only deviation of our data from the SLBLD model, possibly due to specific details of the present system surface energies or to experimental limitations. For example, oxygen impurities tend to locally lower the surface energy of the film, therefore acting as surfactant species[25] competing with Ag. Although the present results do not allow us to get direct information concerning the atomic processes driving the segregation of consecutive Ag layers, our data are compatible with the mechanism of upward Ag diffusion at the walls of pin-holes which put in communication the substrate with the surface of the film.[12–14]

*Also at the Department of Physics, University of Ljubljana, Slovenia.

†Also at the Department of Physics, University of Trieste, Italy.

‡Electronic address: Canepa@fisica.unige.it

[1] W. F. Egelhoff, Jr., Phys. Rev. Lett. **59**, 559 (1987); Z. Q. Qiu, J. Pearson, and S. D. Bader, Phys. Rev. B **49**, 8797 (1994); F. Ciccacci, and S. De Rossi, *ibid.* **51**, 11538 (1995); A. Berger and H. Hopster, Phys. Rev. Lett. **76**, 519 (1996); C. Sommers, J. Zabloudil, C. Uiberacker, P. Weinberger, and L. Szunyogh, Phys. Rev. B **58**, 5539 (1998).

[2] J. Unguris, R. J. Celotta, and D. T. Pierce, J. Magn. Magn. Mater. **127**, 205 (1993); R. Persaud, H. Noro, J. A. Venables, Surf. Sci. **401**, 12 (1998); T. Phalet, M. J. Prandolini, W. D. Brewer, P. De Moor, P. Schuurmans, N. Severijns, B. G. Turrell, A. Van Geert, B. Vereecke, and S. Versyck, Phys. Rev. Lett. **86**, 902 (2001); E. D. Tober, P. F. Marks, D. D. Chambliss, K. P. Roche, M. F. Toney, A. J. Kellock, and R. F. C. Farrow, Appl. Phys. Lett. **77**, 2728 (2000).

[3] R. N. Nogueira and H. M. Petrilli, Phys. Rev. B **60**, 4120 (1999).

[4] W. F. Egelhoff, Jr., Mater. Res. Soc. Symp. Proc. **229**, 27 (1991).

[5] M. Canepa, E. Magnano, P. Cantini, M. Salvietti, and L. Mattera, Surf. Sci. **352–354**, 36 (1996).

[6] M. H. Langelaar and D. O. Boerma, Surf. Sci. **395**, 131 (1997).

[7] M. Canepa, S. Terreni, P. Cantini, A. Campora, and L. Mattera, Phys. Rev. B **56**, 4233 (1997).

[8] D. E. Bürgler, C. M. Schmidt, D. M. Schaller, F. Meisinger, R. Hofer, and H.-J. Güntherodt, Phys. Rev. B **56**, 4149 (1997).

[9] Z. Q. Qiu, J. Pearson, and S. D. Bader, Phys. Rev. Lett. **70**, 1006 (1993); D. M. Schaller, D. E. Bürgler, C. M. Schmidt, F. Meisinger, and H.-J. Güntherodt, Phys. Rev. B **59**, 14516 (1999).

[10] M. Canepa, P. Cantini, O. Ricciardi, S. Terreni, and L. Mattera, Surf. Sci. **429**, 34 (1999).

[11] P. J. Schmitz, W.-Y. Leung, G. W. Graham, and P. A. Thiel, Phys. Rev. B **40**, 11477 (1989); G. W. Graham, P. J. Schmitz, and P. A. Thiel, *ibid.* **41**, 3353 (1989).

[12] A. K. Schmid, D. Atlan, H. Itoh, B. Heinrich, T. Ichinokawa, and J. Kirschner, Phys. Rev. B **48**, 2855 (1993).

[13] S.-L. Chang, J.-M. Wen, P. A. Thiel, S. Gynther, J. A. Meyer and R. J. Behm, Phys. Rev. B **53**, 13747 (1996).

[14] L. D. Roelofs, D. A. Chipkin, C. J. Rockwell, and R. J. Behm, Surf. Sci. Lett. **524**, L89 (2003).

[15] C. S. Fadley, *The Study of Surface Structures by Photoelectron*

Diffraction and Auger Electron Diffraction in Synchrotron Radiation Research: Advances in Surface and Interface Science, Vol. 1: Techniques, edited by R. Z. Bachrach (Plenum, New York, 1992); W. F. Egelhoff, Jr., in *Ultrathin Magnetic Structures I*, edited by J. A. C. Bland and B. Heinrich (Springer-Verlag, Berlin, 1994) Chap. 5.1 p. 220.

[16] L. Floreano, G. Naletto, D. Cvetko, R. Gotter, M. Malvezzi, L. Marassi, A. Morgante, A. Santaniello, A. Verdini, F. Tommasini, and G. Tondello, Rev. Sci. Instrum. **70**, 3855 (1999); R. Gotter, A. Ruocco, A. Morgante, D. Cvetko, L. Floreano, F. Tommasini, and G. Stefani, Nucl. Instrum. Methods Phys. Res. A **467–468**, 1468 (2001).

[17] E. Vlieg, J. Appl. Crystallogr. **33**, 401 (2000). The software is freely distributed at http://www.esrf.fr/computing/scientific/.

[18] F. Bruno, L. Floreano, A. Verdini, D. Cvetko, R. Gotter, A. Morgante, M. Canepa, and S. Terreni, J. Electron Spectrosc. Relat. Phenom. **127**, 85 (2002); cond-mat/0204404 (unpublished).

[19] Y. Chen, F. J. Garcia de Abajo, A. Chassé, R. X. Ynzunza, A. P. Kaduwela, M. A. van Hove, and C. S. Fadley, Phys. Rev. B **58**, 13121 (1998).

[20] F. Bruno, S. Terreni, L. Floreano, A. Cossaro, D. Cvetko, P. Luches, L. Mattera, A. Morgante, R. Moroni, M. Repetto, A. Verdini, and M. Canepa, Phys. Rev. B **66**, 045402 (2002).

[21] H. Li and B. P. Tonner, Phys. Rev. B **40**, 10241 (1989).

[22] J. M. Roussel, A. Saúl, G. Tréglia, and B. Legrand, Phys. Rev. B **55**, 10931 (1997).

[23] J. M. Roussel, A. Saúl, G. Tréglia, and B. Legrand, Phys. Rev. B **60**, 13890 (1999).

[24] B. Aufray, H. Giordano, B. Legrand, and G. Tréglia, Surf. Sci. **331–333**, 805 (1995).

[25] P. Bonanno, M. Canepa, P. Cantini, R. Moroni, L. Mattera, and S. Terreni, Surf. Sci. **454–456**, 697 (2000).